

Electronic Supplementary Information

(ESI)

**Silver nanoparticles supported on nitrogen-doped grapheme
aerogel composite catalyst for oxygen reduction reaction in
aluminum air batteries**

Shihua Li^{a, b}, He Miao^{a*}, Qing Xu^b, Yejian Xue^a, Shanshan Sun^a, Qin Wang^a,

Zhaoping Liu*

^a Key Laboratory of Graphene Technologies and Applications of Zhejiang Province, Ningbo Institute of Materials Technology and Engineering (NIMTE), Chinese Academy of Sciences, Zhejiang 315201, China

^b The School of Material Science and Chemical Engineering, Ningbo University, Zhejiang 315211, P. R. China

Tel.: +86-574-8668-8363

Fax: +86-574-8668-5096

E-mail: liuzp@nimte.ac.cn

E-mail: miaohe@nimte.ac.cn

Experimental section

Materials

Graphite (80 μ m), KMnO₄ (AR), KNO₃ (AR), H₂SO₄ (98%), AgNO₃ (AR), NH₃ (25%~28%), KOH (85.0%) and Ag were purchased from Sinopharm Chemical Reagent Co. Ltd. or Aldrich. All chemicals were used without further purification unless otherwise noted.

Synthesis of N-RGO, Ag/RGO, Ag/C and Ag/N-RGO

Graphene oxide (GO) was prepared from natural graphite flakes using a modified Hummers method.¹ The composite of Ag/N-RGO was prepared by hydrothermal assembly of GO, AgNO₃, and ammonia, subsequently combining with freeze-drying. In a typical experiment, 100 mg AgNO₃ in 10 mL deionized water (DI water) and superfluous ammonia were mixed to form a uniform and transparent silver-ammonia solution. 20 mL of GO dispersion (5mg/mL) was added into the silver-ammonia solution and stirred thoroughly to form a stable aqueous suspension by sonication for 30 min. Subsequently, the stable suspension was sealed in a Teflon-lined autoclave and hydrothermally treated at 180 °C for 6 h to prepare the N-doped graphene-based 3D hydrogel. Then, the as-prepared sample was freeze-dried for two days, and named as Ag/N-RGO. For optimization of the compositions of Ag/N-RGO composites, the mass ratios of AgNO₃/RGO were tailored as 0, 0.5, 1 and 2 during the preparation of Ag/N-RGO.

For comparison, Ag nanoparticles supported on the reduced graphene oxide sheets (Ag/RGO) and carbon black (Ag/C) were also prepared via the same procedure. The synthetic procedure of Ag/RGO was almost same with that of Ag/N-RGO except for the addition of ammonia. In the case of the preparation of Ag/C, the carbon black (Vulcan XC-72) was used to instead of GO and the other steps kept unchanged comparing with the synthetic procedure of Ag/RGO. For the preparation of Nitrogen doped graphene (N-RGO), AgNO₃ solution was not used following the same synthetic procedure of Ag/N-RGO. In addition, the mixture of Ag+N-RGO was made by mixing Ag and N-RGO with the mass ratio of 1:9.

Characterizations

The morphologies and structures of the samples were observed by a Hitachi S-4800 field emission scanning-electron microscope (SEM) and a JEOL JEM-2100 Transmission electron microscopy (TEM). X-ray diffraction (XRD) measurements were performed on an AXS D8 Advance diffract meter using Cu K α radiation at a scanning rate of 0.02° s⁻¹ from 10° to 80°. X-ray photoelectron spectra (XPS) were recorded by an AXISULTARDLD spectroscopy with an Al/K α X-ray source.

Electrochemical measurements

For electrode preparation, 10 mg sample and 5 mg carbon (Vulcan XC-72) were dispersed in 2 mL absolute ethyl alcohol with 90 μ L Nafion (5%, Dupont) and ultrasonically blended for 1h to form a well-dispersed ink. Then, 10 μ L portion of the ink suspension was slightly dropped on the disk surface of the pre-polished glassy carbon electrode. The electrodes were dried at room temperature. For comparison, a commercially available catalyst of 20%Pt/C (Johnson Matthey Corp.) was used as the benchmark.

Linear sweep voltammetry (LSV) and cyclic voltammetry (CV) measurements were performed on a rotating disk electrode (RDE, 0.196cm², Pine, American) by a computer-controlled electrochemical workstation (CHI 1040B) with a three-electrode system in a 0.1 molL⁻¹ KOH aqueous solution at room temperature. The glass carbon electrode (RDE) loading with the electrocatalyst, Hg/HgO electrode and Pt wire was used as the working electrode, reference electrode and counter electrode, respectively. The cyclic voltammetry curves (CVs) were scanned from +0.5 V to -0.4 V, and recorded at a scan rate of 5 mV s⁻¹ in the O₂-saturated 0.1 molL⁻¹ KOH solution at the room temperature. The linear sweep voltammetry curves (LSVs) were scanned from +0.2 V to -0.8 V, and recorded at a scan rate of 5 mV s⁻¹ in the O₂-saturated 0.1 molL⁻¹ KOH solution at the room temperature. The rotation rate of the disk was varied between 400 and 2400 rpm. The electron transferred number (n) per oxygen molecule in the ORR process was calculated by the Koutechy-Levich (K-L) equation (equation (1)~(3))² :

$$\frac{1}{J} = \frac{1}{J_k} + \frac{1}{J_L} = \frac{1}{J_k} + \frac{1}{B\omega^{1/2}} \quad (1)$$

$$B = 0.62nFkD_0^{1/3}C_0\nu^{-1/6} \quad (2)$$

$$J_k = nFkC_0 \quad (3)$$

where J_k and J_L represent kinetics and diffusion limiting current densities (mA cm^{-2}) respectively; n is the overall electron transferred number; F is the Faraday constant (96485 C mol^{-1}); k is the rate constant for ORR (m s^{-1}); D_0 is the diffusion coefficient of O_2 in $0.1 \text{ mol L}^{-1} \text{ KOH}$ ($1.9 \times 10^{-9} \text{ m}^2 \text{ s}^{-1}$); C_0 is the saturation concentration of O_2 (1.2 mol m^{-3}); ν is the kinetic viscosity of solution ($1 \times 10^{-6} \text{ m}^2 \text{ s}^{-1}$), and ω is the rotation rate (rad s^{-1}).

RRDE measurements were carried out at a scan rate of 5 mV s^{-1} in the potential range from $+0.2 \text{ V}$ to -0.8 V at 1600 rpm in the O_2 -saturated $0.1 \text{ mol L}^{-1} \text{ KOH}$ solution at the room temperature. The electron transfer number (n) and the peroxide percentage ($X_{\text{HO}_2^-}$) were calculated by the following equation³:

$$n = \frac{4I_D}{I_D + \left(\frac{I_R}{N}\right)} \quad (4)$$

$$X_{\text{HO}_2^-} [\%] = 100 \frac{\frac{2I_{\text{ring}}}{N}}{I_{\text{disk}} + \frac{I_{\text{ring}}}{N}} \quad (5)$$

where I_{disk} , I_{ring} , n , N were the disk current, ring current, number of electrons transferred per oxygen molecule, current collection efficiency of the Pt ring, respectively.

Amperometric i - t curves were applied to assess the durability of the as-prepared catalyst toward ORR in O_2 -saturated $0.1 \text{ mol L}^{-1} \text{ KOH}$ electrolyte at -0.6 V for 40000 s at the rotation rate 1600 rpm . Electrochemical impedance spectra (EIS) were recorded by CHI660e electrochemical workstation in the frequency range from 100 kHz to 0.1 Hz with an AC signal amplitude of 5 mV in O_2 -saturated $0.1 \text{ mol L}^{-1} \text{ KOH}$ electrolyte.

The ORR activities were calculated at 0.9 V vs. RHE based on the following equation⁴:

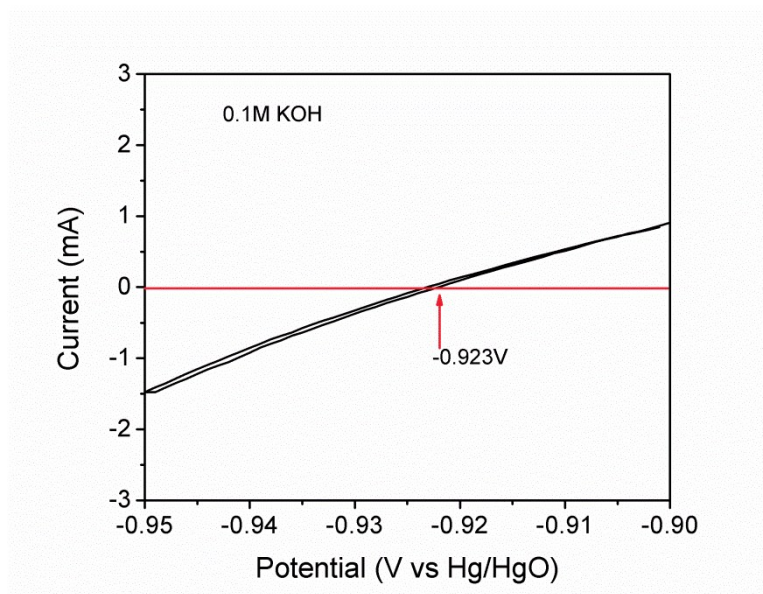
$$i_k = \frac{i * i_d}{i_d - i} \quad (6)$$

$$\text{mass activity} = \frac{i_k}{m} \quad (7)$$

where m is the amount of Ag loading, i is the experimentally measured current, i_d is the diffusion-limiting current, and i_k is the kinetic current.

RHE calibration

Hg/HgO electrode was used as the reference electrode in our measurements. We calibrated our Hg/HgO reference electrode with respect to reversible hydrogen electrode (RHE). The calibration was performed in the high purity hydrogen saturated 0.1M KOH electrolyte with a Pt plate as the working electrode. CVs were run at a scan rate of 1 mV s^{-1} , and the average of the two potentials at which the current crossed zero was taken to be the thermodynamic potential for the hydrogen electrode reaction.



So in 0.1 M KOH, $E(\text{RHE}) = E(\text{Hg/HgO}) + 0.923 \text{ V}$.

Aluminum-air (Al-air) battery fabrications and tests

Aluminum-air batteries were fabricated and tested for the polarization curves on a multichannel battery testing system (CT2001A, Land Company) at about 30°C . The as-synthesized catalysts were used in the cathode. The cathode was fabricated with a

three-layer structure including the catalytic layer, current collector layer and gas diffusion layer. The current collector layer and the gas diffusion layer were nickel foam and porous PTFE film with a 4cm×4cm square area, respectively. The catalytic layer was prepared in the following sequence: (i) 0.48g as-prepared catalyst, 0.83g active carbon and 0.23g acetylene black were mixed in a beaker with 50ml ethyl alcohol and then the mixture was stirred magnetically to obtain a homogeneous solution; (ii) 0.67g PTFE emulsion (60wt%) was added into the solution and stirred for further 30min; (iii) the beaker was then transferred into a water-bath with stirring under 80°C until the ethyl alcohol was evaporated and the slurry formed a paste; (iv) the paste was rolled into a 0.35mm of film with a square area of 4cm × 4cm. The catalytic layer was placed on the nickel foam, and pressed with a pressure of 20MPa for 2 minutes, followed by the sintering at 340°C for 30 minutes. Then, the above two-layer architecture was placed on the porous PTFE film, and pressed with a pressure of 10MPa for 2 minutes at 150°C. Aluminum-air batteries with an active area of 2×2 cm² were fabricated with the as-prepared air cathodes and tested by a homemade testing device. The aluminum plate and 4 molL⁻¹ KOH aqueous solution were used as the anode and electrolyte, respectively. The Al-Mg-Sn-Ga quaternary Al alloy was used as the anode, and the distance between anode and cathode is 8-10mm. I-V discharge curves were recorded at about 30 °C.

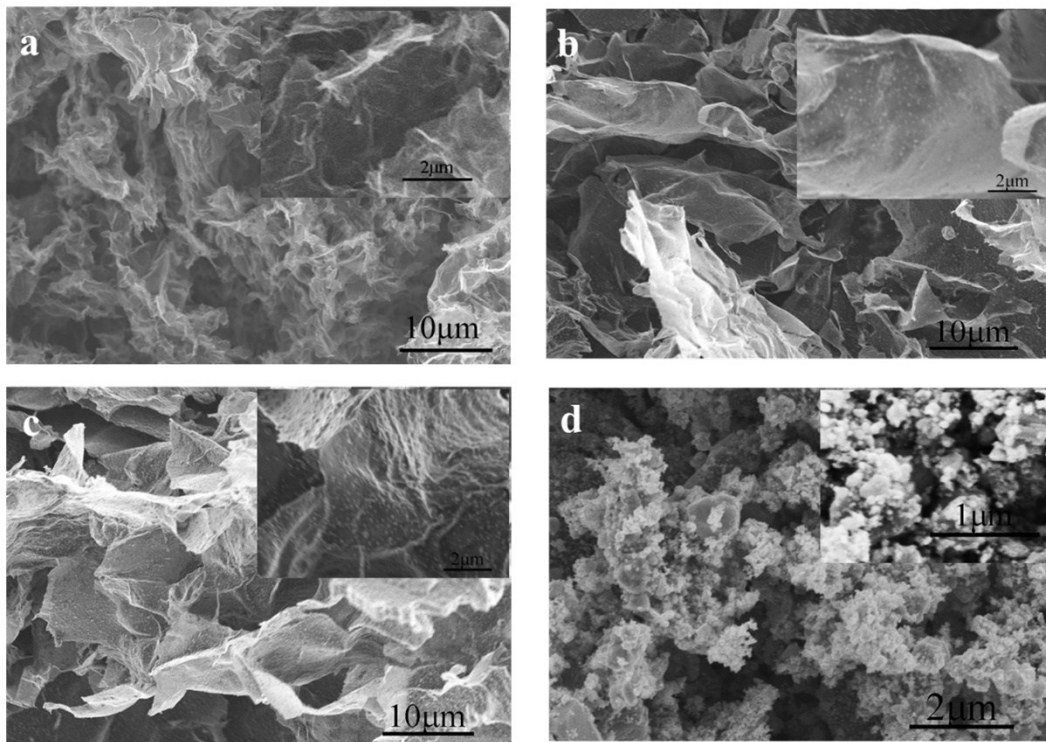


Fig. S1. SEM images of the silver supported on N-RGO with the different mass ratios: (a) $m(\text{AgNO}_3)/m(\text{GO})=0$; (b) $m(\text{AgNO}_3)/m(\text{GO})=0.5$; (c) $m(\text{AgNO}_3)/m(\text{GO})=2$; (d) $m(\text{AgNO}_3)/m(\text{GO})=10$.

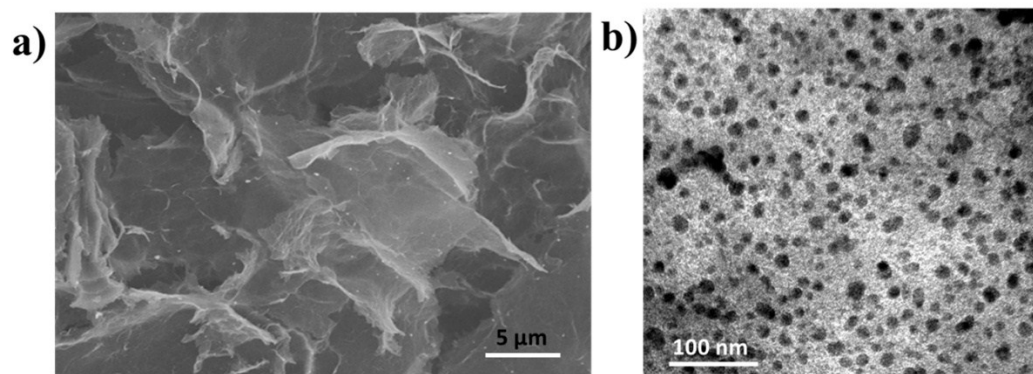


Fig. S2. SEM (a) and TEM (b) images of the as-prepared Ag/RGO.

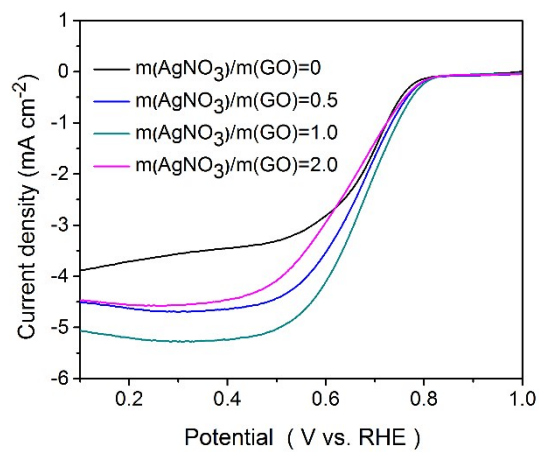


Fig S3. Linear-sweep voltammogram curves of the silver supported on N-RGO with the different mass ratios. Electrolyte: oxygen-saturated 0.1 mol L⁻¹ KOH, scan rate: 5 mV s⁻¹, and rotation speed: 1600rpm.

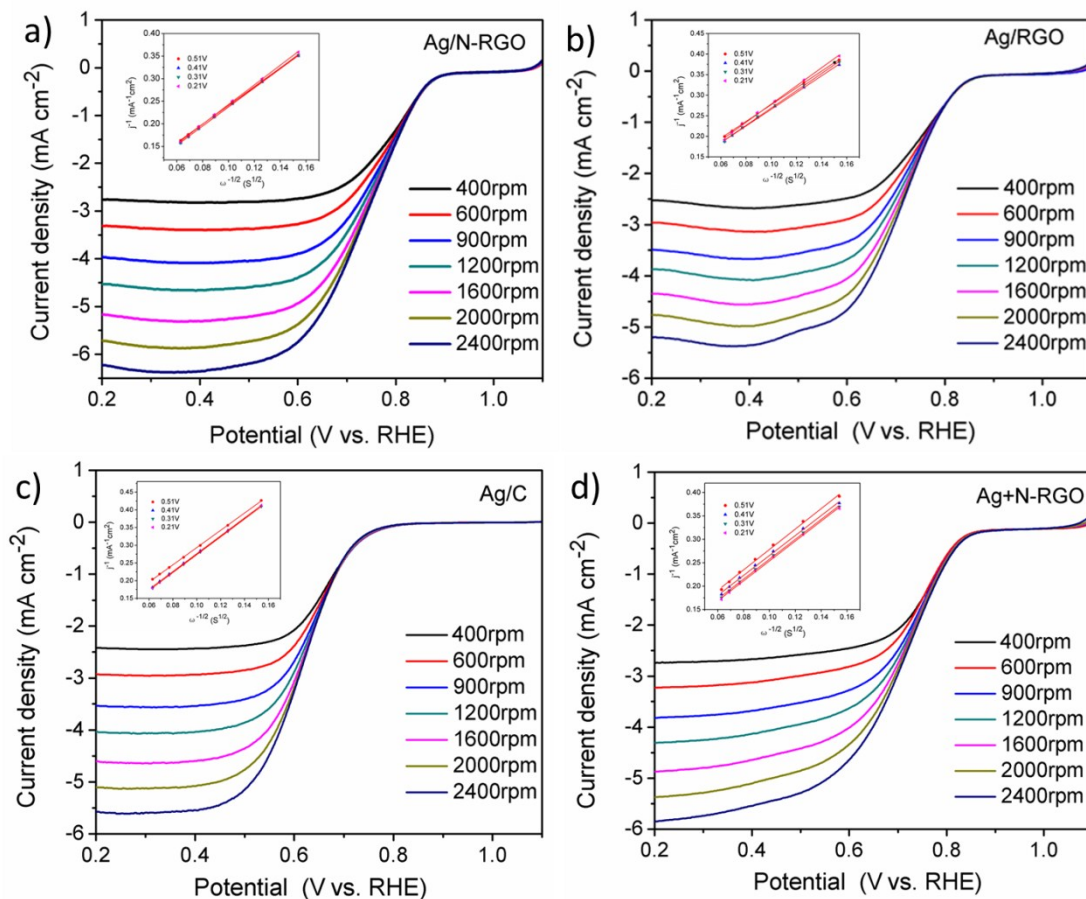


Fig. S4. LSV curves at different rotation speed from 400 to 2400 rpm and K-L plots at different potential from 0.21V to 0.51V of Ag/N-RGO (a), Ag/RGO (b), Ag/C (c) and Ag+N-RGO (d). Electrolyte: O_2 -saturated $0.1 \text{ mol L}^{-1} \text{ KOH}$, scan rate: 5 mV s^{-1} .

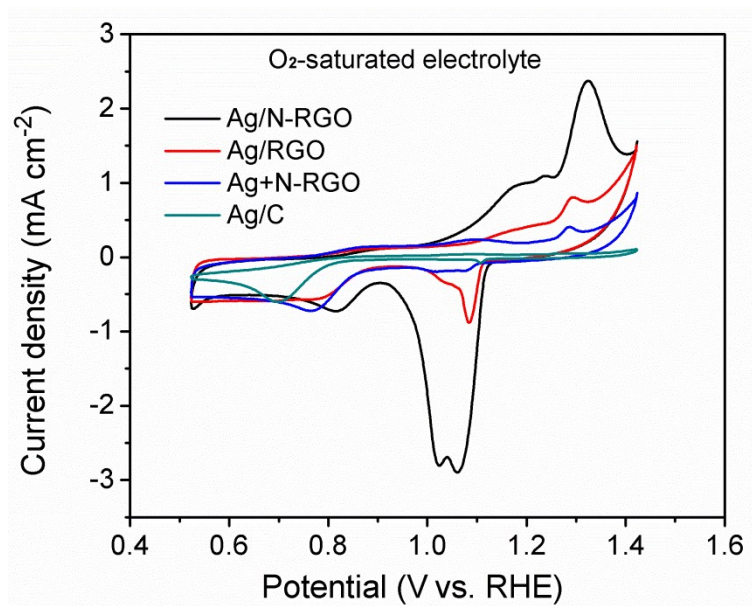


Fig. S5. CV curves of Ag/N-RGO, Ag/RGO, Ag+N-RGO and Ag/C. Electrolyte: O₂-saturated 0.1 mol L⁻¹ KOH, scan rate: 5 mV s⁻¹.

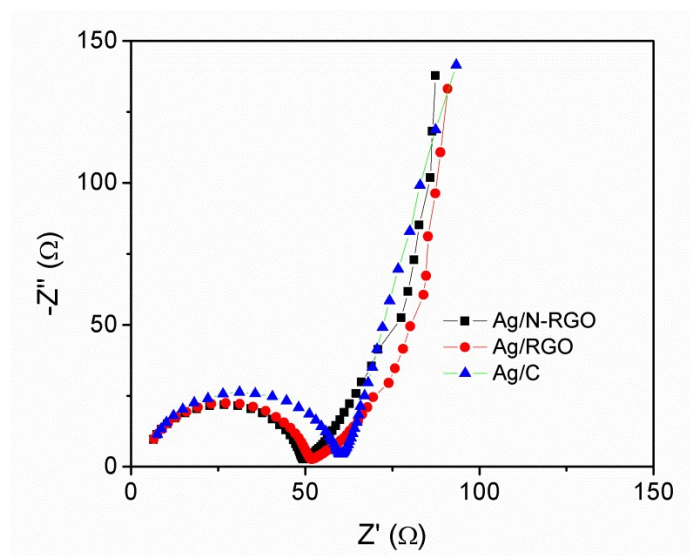


Fig. S6. Nyquist plots of EIS for Ag/N-RGO, Ag/rGO and Ag/C in O₂-saturated 0.1 mol L⁻¹ KOH.

Table S1. Element contents of RGO, N-RGO, Ag/RGO, Ag/C and Ag/N-RGO.

catalysts	Species concentration (wt. %)			
	C	O	N	Ag
RGO	82.3	17.7	—	—
N-RGO	79.0	13.5	7.5	—
Ag/RGO	72.3	13.8	—	13.9
Ag/N-RGO	70.4	11.6	6.8	11.2
Ag/C	87.9	—	—	12.1

Table S2. Peak positions and percentages of the N species of N 1s spectra for N-RGO and Ag/N-RGO samples.

N Species	N-RGO		Ag/N-RGO	
	Peak position/eV	%N	Peak position/eV	%N
Pyridinic N	398.6	2.4	398.4	4.1
Pyrrolic N	400.0	4.4	399.8	2.0
Graphitic N	401.8	0.7	401.7	0.7

Table S3. Some important parameters derived from LSV curves of Ag/RGO, Ag/N-RGO, Ag/C, Ag+N-RGO, Ag/N-rGO⁵ and Ag NCs/NG⁶ catalysts.

catalysts	E_{onset} (V vs. RHE) ^a	$E_{1/2}$ (V vs. RHE)	J_L (mA cm ⁻²) ^b	Electron transfer number (n) ^c	Mass activity (A/g Ag) ^d	Tafel slope (mV/decade, low j)
Ag/RGO	0.88	0.72	4.5	3.90	2.2	-79
Ag/N-RGO	0.96	0.76	5.3	3.98	5.3	-70
Ag/C	0.79	0.63	4.6	3.60	0.4	-96
Ag+N-RGO	0.95	0.72	4.8	3.96	4.7	-80
Ag/N-rGO ⁵	0.87	0.77	4.9	—	—	—
Ag NCs/NG ⁶	0.80	0.75	2.4	—	—	—

^aPotential at which the ORR current density is 0.1 mA cm⁻². ^bTaken as the current densities at 0.36V vs. RHE. ^cCalculated by Koutecky-Levich equation as the average electron transfer number from 0.21V to 0.51V vs. RHE. ^dCalculated at 0.9V vs. RHE.

References

- 1 H.Cao, X. Zhou, Z. Qin and Z. Liu., *Carbon*, 2013, **56**, 218.
- 2 Y. Lu and W. Chen, *J. Power Sources*, 2012, **197**, 107.
- 3 D. Geng, Y. Chen, Y. Chen, Y. Li, R. Li, X Sun, S. Ye and S. Knights, *Energy . Environ. Sci*, 2011, **4**, 760.
- 4 D. He, Y. Jiang, H. Lv, M. Pan and S. Mu, *Appl. Catal. B: Environmental*, 2013, **132-133**, 379.
- 5 R. Zhou and S. Z. Qiao, *Chem.Mater*, 2014, **26**, 5868.
- 6 S. Jin, M. Chen, H. Dong, B. He, H. Lu, L. Su, W. Dai, Q. Zhang and X. Zhang, *J. Power Sources*, 2015, **274**, 1173.